Numerical Methods in Engineering Simulation

Editors:

M. Cerrolaza
Universidad Central de Venezuela, Venezuela

C. Gajardo
Universidad de Los Andes, Venezuela

C.A. Brebbia
Wessex Institute of Technology, UK

Computational Mechanics Publications
Southampton Boston

Combined convection-radiation effects in the entry region of parallel plate channels: a preliminary study

A. Sánchez,[a] P. Guillén,[a] D.A. Muñoz,[a] C.M. Ramírez,[a]
A. Campo[b]

[a] *Escuela de Ingeniería Mecánica, Universidad de Los Andes, Mérida 5101, Venezuela*

[b] *College of Engineering, Idaho State University, Pocatello, Idaho, USA*

ABSTRACT

In the present work a numerical model that allows for the simulation of the combined conductive, convective, and radiative effects that take place in the entrance region of channels formed by two plane parallel plates is described. The model is two–dimensional; it includes the possibility of considering participating or transparent media, and allows for a wide variety of boundary conditions. In this paper the model has been applied to the simulation of the hydrodynamic and thermal development that takes place when a cold fluid enters a channel formed by two hot isothermal walls.

For this preliminary study, no grid independent solution was sought and the results given are for a fixed 24 by 26 mesh. This mesh size is enough to show the validity of the model and the relative tendencies of the different Nusselt numbers that are presented in the form of plots.

It is concluded that the numerical model produces plausible results and that the mechanism of radiative heat exchange strongly affects the heat transfer process that takes place in the entrance region of this type of channels. Finally, in view of these findings, a more detailed study aimed at obtaining grid independent solutions for all type of boundary conditions is recommended.

INTRODUCTION

In a parallel-plate channel, the idealization that the velocity profile is fully developed occurs when the dimensionless hydrodynamic entry length, X/H, is greater than about 0.022 Re. On the one hand, for Prandtl number fluids greater than about 5, the velocity profile develops much faster than the temperature profile even if both velocity and temperature are uniform at the channel entrance, so that the fully developed velocity idealization introduces little error. On the other hand, whenever the Prandtl numbers are less than 5, the temperature profile develops more rapidly than the velocity profile, and the simplistic fully developed idealization is invalidated for a thermal-entry-length solution. The latter is precisely the situation in cooling channels of electronic components where the working fluid is air (Pr = 0.7), and the chips (heating elements) are uniformly attached to the channel plates from the entrance to the exit.

A brief literature review related to the above-cited problem will be delineated in the following paragraphs. Simultaneous development of velocity and temperature inside parallel-plate channels was first investigated by Sparrow [1] for equal surface temperatures. This author used Schiller's velocity profile and employed the Kármán-Pohlhausen integral method. Murakawa [2] considered the combined entry length problem, but did not present exact solutions of the momentum and energy equations. Stephan [3] employed an approximate series solution for the problem treated in [1,2], and constructed a reliable correlation equation for the average Nusselt number for a wide spectrum of Prandtl number fluids. Hwang and Fan [4] obtained an all-numerical finite-difference solution and reported the results in terms of a mean Nusselt number equation for Pr ranging between 0.01 and 50. Mercer et al. [5] also solved the same finite-differences problem using the vorticity stream function representation, and also validated the theoretical predictions with experiments. The structure of the proposed average Nusselt correlation equation was similar to the one proposed by Stephan [3].

In practical thermal systems it is nearly always the case that radiation acts in conjunction with convection, and the two heat transfer mechanisms must be accounted for simultaneously. If the flowing medium is air, the assumption of a transparent, or non-participating medium is often justified. A limited number of publications have investigated combined convection and radiation for flowing medium inside a parallel-plate channel. Representative references are those by Viskanta [6] (assuming fully developed velocity and temperature profiles), Kurosaki [7] (assuming fully developed velocity profile and one dimensional conduction and radiation), Keshock and Siegel [8] and Lin and Thorsen [9] (the most notorious simplification in the analysis pertains to the assumption that the convective heat transfer coefficient, h, between the channel surfaces and the fluid is constant and known a priori).

In view of the preceding review, the primary goal of this investigation was to develop a complete numerical model that removes the restrictions imposed in previous works [6-9]. This model will be applied, in the future, to the prediction of the cooling requirements of electronic elements by combined forced convection and radiation.

In the present work the 2-D model, without restrictions, is developed and some preliminary tests are performed. The results reported here are qualitatively sound and indicate the path for the continuation of this investigation toward the finding of benchmark solutions.

GEOMETRY

The geometry used in this numerical study is shown in Figure 1.

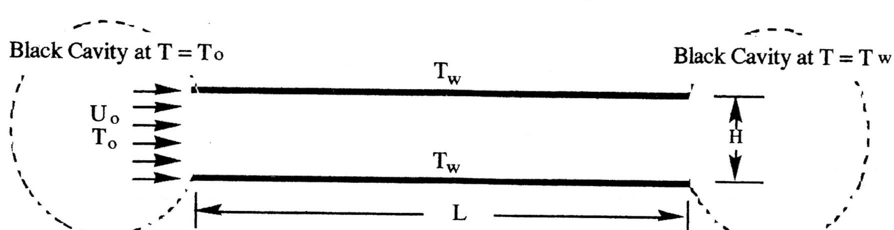

Figure 1. Geometry

The upper and lower plates are considered isothermal, both plates are at the same temperature T_w, and all surfaces are considered diffuse and black emitters. The fluid enters the channel with constant velocity (U_o) and constant temperature (T_o), and the spacing between the plates is H<<L.

MATHEMATICAL MODEL

The problem is governed by the equations and boundary conditions presented next.

The Transport Equations

The transport equations for a simple fluid in a 2-D setting can be written as follows [10].
Continuity:

$$\frac{\partial}{\partial x}(\rho u) + \frac{\partial}{\partial y}(\rho v) = 0 \qquad (1)$$

x Momentum:

$$\frac{\partial}{\partial x}(\rho\, u\, u) + \frac{\partial}{\partial y}(\rho\, u\, v) = \frac{\partial}{\partial x}\left(\mu\, \frac{\partial u}{\partial x}\right) + \frac{\partial}{\partial y}\left(\mu\, \frac{\partial u}{\partial y}\right) - \frac{\partial P}{\partial x} \tag{2}$$

y Momentum:

$$\frac{\partial}{\partial x}(\rho\, u\, v) + \frac{\partial}{\partial y}(\rho\, v\, v) = \frac{\partial}{\partial x}\left(\mu\, \frac{\partial v}{\partial x}\right) + \frac{\partial}{\partial y}\left(\mu\, \frac{\partial v}{\partial y}\right) - \frac{\partial P}{\partial y} \tag{3}$$

Energy:

$$\frac{\partial}{\partial x}(\rho\, u\, T) + \frac{\partial}{\partial y}(\rho\, v\, T) = \frac{\partial}{\partial x}\left(\frac{k}{Cp}\frac{\partial T}{\partial x}\right) + \frac{\partial}{\partial y}\left(\frac{k}{Cp}\frac{\partial T}{\partial y}\right) + Q - \nabla q_r \tag{4}$$

Subjected to the following boundary conditions (when both plates are isothermal and maintained at the same temperature):

$$\begin{array}{lll} x = 0 & \forall\, y & u = U_o;\quad v = 0;\quad T = T_o \\ \forall\, x & y = H & u = 0;\quad v = 0;\quad T = T_w \\ \forall\, x & y = 0 & u = 0;\quad v = 0;\quad T = T_w \end{array} \tag{5}$$

Also important for the completion of the model are the expressions for the wall heat fluxes per unit area acting, due to convection, over the lower (q_{cl} in $y = 0$) and upper (q_{cu} in $y=H$) plates:

$$q_{cl} = -k\left.\frac{\partial T}{\partial y}\right|_{y=0} \quad \text{and} \quad q_{cu} = -k\left.\frac{\partial T}{\partial y}\right|_{y=H} \tag{6}$$

In Equations 1-6 the fluid properties are considered constant and are designated as ρ for density, μ for dynamic viscosity, α for thermal diffusivity, Cp for specific heat, and k for thermal conductivity. Also in Equations 1-6, P stands for pressure, T for temperature, and u and v for the velocity components in the x and y directions respectively.

After introducing the parameters:

$$\begin{array}{llll} \xi = \dfrac{x}{H} & \eta = \dfrac{y}{H} & \bar{u} = \dfrac{u}{U_o} & \bar{v} = \dfrac{v}{U_o} \\ \theta = \dfrac{T}{T_o} & Re = \dfrac{\rho\, U_o H}{\mu} & Pr = \dfrac{\mu}{\rho\, \alpha} & \alpha = \dfrac{k}{\rho\, Cp} \\ \bar{P} = \dfrac{P}{\rho\, u^2} & \bar{Q} = Q\dfrac{H^2}{kT_o} & \nabla \bar{q}_r = \nabla q_r \dfrac{H^2}{kT_o} & \bar{q}_c = q_c \dfrac{H}{kT_o} \end{array} \tag{7}$$

the transport equations become:

Continuity:

$$\frac{\partial}{\partial \xi}\left(\bar{u}\right) + \frac{\partial}{\partial \eta}\left(\bar{v}\right) = 0 \tag{8}$$

x Momentum:

$$\frac{\partial}{\partial \xi}\left(\bar{u}\,\bar{u}\right) + \frac{\partial}{\partial \eta}\left(\bar{u}\,\bar{v}\right) = \frac{1}{Re}\left[\frac{\partial}{\partial \xi}\left(\frac{\partial \bar{u}}{\partial \xi}\right) + \frac{\partial}{\partial \eta}\left(\frac{\partial \bar{u}}{\partial \eta}\right)\right] - \frac{\partial \bar{P}}{\partial \xi} \tag{9}$$

y Momentum:

$$\frac{\partial}{\partial \xi}\left(\bar{v}\ \bar{u}\right) + \frac{\partial}{\partial \eta}\left(\bar{v}\ \bar{v}\right) = \frac{1}{Re}\left[\frac{\partial}{\partial \xi}\left(\frac{\partial \bar{v}}{\partial \xi}\right) + \frac{\partial}{\partial \eta}\left(\frac{\partial \bar{v}}{\partial \eta}\right)\right] - \frac{\partial \bar{P}}{\partial \eta} \tag{10}$$

Energy:

$$\frac{\partial}{\partial \xi}\left(\bar{u}\ \theta\right) + \frac{\partial}{\partial \eta}\left(\bar{v}\ \theta\right) = \frac{1}{RePr}\left[\frac{\partial}{\partial \xi}\left(\frac{\partial \theta}{\partial \xi}\right) + \frac{\partial}{\partial \eta}\left(\frac{\partial \theta}{\partial \eta}\right) + \bar{Q} - \nabla\ \bar{q}_r\right] \tag{11}$$

Subjected to the following boundary conditions:

$$\begin{array}{llll} \xi = 0 & \forall\ \eta & \bar{u} = 1;\quad \bar{v} = 0; & \theta = 1 \\ \forall\ \xi & \eta = 1 & \bar{u} = 0;\quad \bar{v} = 0; & \theta = \theta_w \\ \forall\ \xi & \eta = 0 & \bar{u} = 0;\quad \bar{v} = 0; & \theta = \theta_w \end{array} \tag{12}$$

and the convection heat fluxes per unit area:

$$\bar{q}_{cl} = \ = -\left.\frac{\partial \theta}{\partial \eta}\right|_{\eta = 0} \quad \text{and} \quad \bar{q}_{cu} = \ = -\left.\frac{\partial \theta}{\partial \eta}\right|_{\eta = 1} \tag{13}$$

In Equations 8-13 Re is the Reynolds number; Pr is the Prandtl number; ξ and η are dimensionless coordinates; $\bar{Q}$ is the dimensionless heat generation; $\nabla\ \bar{q}_r$ is the dimensionless divergence of the radiative heat flux vector; and $\bar{u}$, $\bar{v}$, and θ are the dimensionless ξ velocity component, the dimensionless η velocity component, and the dimensionless temperature respectively.

The Radiation Model

The radiative exchange algorithm used in this study is based on the discrete ordinates method described elsewhere [10].

The radiative transfer equation (ETR), describing the propagation of radiation intensity (I) along a line of sight (ζ), can be written as:

$$\frac{dI}{d\zeta} = -\ \beta I(\zeta) + a\, I_b \tag{14}$$

where β is the extinction coefficient representing the added effects of the monochromatic absorption coefficient (a) and the scattering coefficient (s), if they are present.

Equation 14 is subjected to the following boundary conditions:

$$I^+ = \varepsilon I_b^+ + \frac{v}{\pi}\int_0^{2\pi} I^-(\bar{\omega}_i)\ \delta\ d\omega^- + \tau_t\ I_{ba}^+ \tag{15}$$

The divergence of the radiative heat flux vector is given by the following expression:

$$\nabla \cdot q_r = a\ 4\pi\ I_b - a\int_0^{4\pi} I(\bar{\omega})\ d\omega \tag{16}$$

The radiative heat flux per unit area acting upon a given surface is given as:

$$q_r = \int_{4\pi} I \, \delta \, d\omega \tag{17}$$

After introducing the parameters:

$$\Phi = \theta^4 = \frac{T^4}{T_o^4} \qquad \bar{\zeta} = \frac{\zeta}{H} \qquad \tau_o = a\,H$$

$$N = \frac{k}{H\sigma T_o^3} \qquad \text{and} \qquad \bar{q}_r = q_r \frac{H}{kT_o} \tag{18}$$

in the absence of scattering effects, Equations 14-17 become:

$$\frac{d\Phi}{d\bar{\zeta}} = \tau_o \left(\Phi_b - \Phi \right) \tag{19}$$

$$\Phi^+ = \varepsilon \, \Phi_b^+ + \frac{\nu}{\pi} \int_0^{2\pi} \Phi^-(\bar{\omega}_i) \, \delta \, d\omega^- + \tau_t \, \Phi_{ba}^+ \tag{20}$$

$$\nabla \bar{q}_r = \frac{1}{\pi N} \left[\tau_o \left(4\pi \, \Phi_b - \int_0^{4\pi} \Phi(\bar{\omega}) \, d\omega \right) \right] \tag{21}$$

$$\bar{q}_r = \frac{1}{\pi N} \int_{4\pi} \Phi \, \delta \, d\omega \tag{22}$$

The different dimensionless quantities appearing in Equations 19-22 stand for: Φ the intensity; $\bar{\zeta}$ the line of sight direction; τ_o the optical thickness; ε, ν, and τ_t the surface emissivity, reflectivity, and transmissivity respectively; ω the solid angle along $\bar{\zeta}$; δ is the angle formed between $\bar{\zeta}$ and the normal to the surface; N is the conduction-radiation parameter as defined in Equation 18 (in the literature it is more common to find $\bar{N}$ = N/4). The subindexes b and ba indicate black and background respectively.

Local Nusselt Numbers

The convective Nusselt number at any given location x (Nu_{xc}) is evaluated as:

$$Nu_{xc} = \frac{q_{cl} + q_{cu}}{(\bar{T}_w - \bar{T}_b)} \tag{23}$$

where $\bar{T}$ is the mean (or bulk) temperature defined as [11]:

$$\bar{T} = \frac{\int_0^H \rho u C_v T \, dy}{\dot{m} C_v} \tag{24}$$

with $\dot{m}$ representing the mass flow rate $(\rho U_o H)$.

The local radiative Nusselt number (Nu_{xr}) is defined next:

$$Nu_{xr} = \frac{-\frac{1}{H}\int_0^H \nabla \cdot q_r \, dy}{(\bar{T}_w - \bar{T}_b)} \tag{25}$$

It should be noticed that the numerator in Equation 25 represents the heat per unit area gained or lost by the fluid, due to radiation alone, as it flows through a given axial location x.

Based on dimensionless quantities, Equations 23 and 25 can be written as:

$$Nu_{xc} = \frac{\bar{q}_{cl} + \bar{q}_{cu}}{(\bar{\theta}_w - \bar{\theta}_b)} \quad \text{and} \quad Nu_{xr} = \frac{-\int_0^1 \nabla \bar{q}_r \, d\eta}{(\bar{\theta}_w - \bar{\theta}_b)} \tag{26}$$

where the subindexes w and b represent wall and bulk, and $\bar{\theta}$ is given by:

$$\bar{\theta} = \int_0^1 \bar{u} \, \theta \, d\eta \tag{27}$$

Total Nusselt Number

The total Nusselt number, accounting for the combined effects of radiation and convection, can be evaluated,at any given location x, from Equation 26 as:

$$Nu_t = Nu_{xc} + Nu_{xr} = \frac{\bar{q}_{cl} + \bar{q}_{cu} - \int_0^1 \nabla \bar{q}_r \, d\eta}{(\bar{\theta}_w - \bar{\theta}_b)} \tag{28}$$

Mean Nusselt Numbers

Mean Nusselt numbers from the entry up to location x (Nu_m) can be defined for both convection ((Nu_{mc}) and radiation (Nu_{mr}) as follows:

$$Nu_{mc} = \frac{1}{x}\int_0^x Nu_{\xi c} \, d\xi \quad \text{and} \quad Nu_{mr} = \frac{1}{x}\int_0^x Nu_{\xi r} \, d\xi \tag{29}$$

NUMERICAL MODELS AND PROCEDURE

The numerical solution of the transport equations was performed by means of a control volume approach [12]. The radiative model, on the other hand, was solved by using a discrete ordinates algorithm that includes the possibility of considering participating media [10].

A personal computer was used for this preliminary study. Given the computer memory and speed limitations, the procedure described next was implemented in order to use a fixed mesh size of 24x26 grids. In all cases, a numerical domain with very large aspect ratio (normally 1:128) was first solved to verify that fully developed conditions where reached. Next, the velocities, temperatures, and intensities from the middle plane of that domain were used as outgoing boundary conditions for a new domain that was half the length of the original domain (1:64). This procedure was repeated as many times as needed in order to get as close to the entry as desired (normally 1:0.5). Sometimes, as a result of the transference of results from a coarse to a finer mesh, unrealistic (oscillating) temperatures or intensities were found. This later shortcoming was overcome by forcing the maximum temperature (if the fluid is being heated) and intensity in any given domain to be at the exit of that domain.

Some initial studies for grid independent solutions seem to indicate the need for at least 60x60 grid elements for a 1:1 domain. This represents, approximately, 60x7500 for the 1:128 domain. It should be noticed, therefore, that the procedure described above could be useful even if a more powerful computer is used.

EXPERIMENTS AND RESULTS

The results from two numerical experiments are presented here. In both cases the Reynolds number is taken as 10, the Prandtl number is taken as 0.72, and the walls, considered black, are at a temperature that is twice that of the entering fluid. In one of the experiments the fluid is considered non participating (producing pure convective results) while in the other experiment the optical depth (τ_0) is taken as 1.0 and the conduction to radiation parameter (N) is taken to be 0.02.

The results are presented in Figures 2 to 4. These figures show, in order, the distribution of bulk temperature, local Nusselt numbers and mean Nusselt numbers plotted against the reciprocal of the Graetz number.

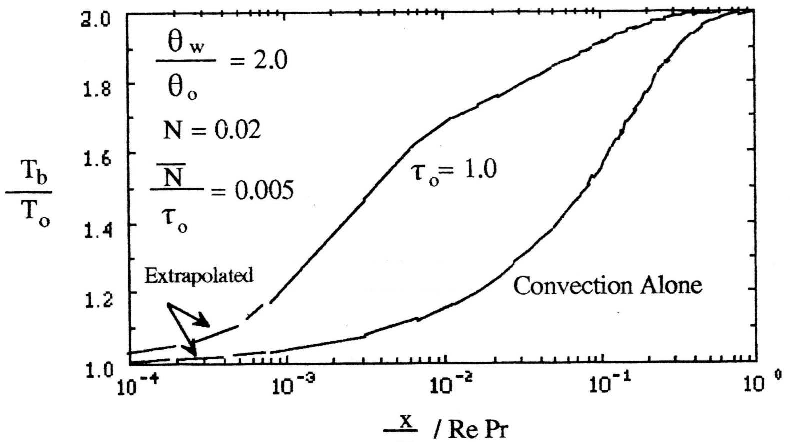

Figure 2. Bulk Temperature development

The results plotted in Figures 2-4 show qualitative good agreement with previously published results –based on simplified analysis– by other authors [4-7]. An important exception to this good qualitative agreement is the distribution of the local Nusselt number in the presence of radiation. It has been previously reported [13] (for fully developed hydrodynamic entry and 1-D radiative transfer calculations) that for the heated wall case, and in the presence of radiation, the local Nusselt number does not reach an asymptotic value. However, the results from the present work show, as can be seen in Figure 3, a clear tendency toward an asymptotic value (Nu ≈ 10) indicating an apparent discrepancy that requires further study.

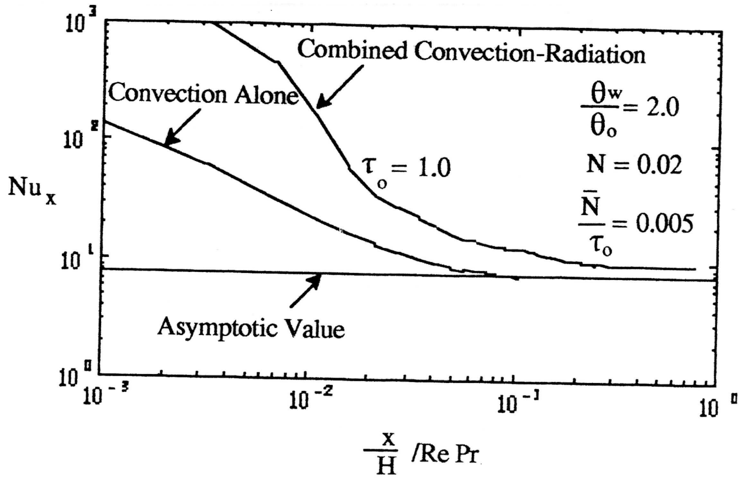

Figure 3. Local Nusselt numbers

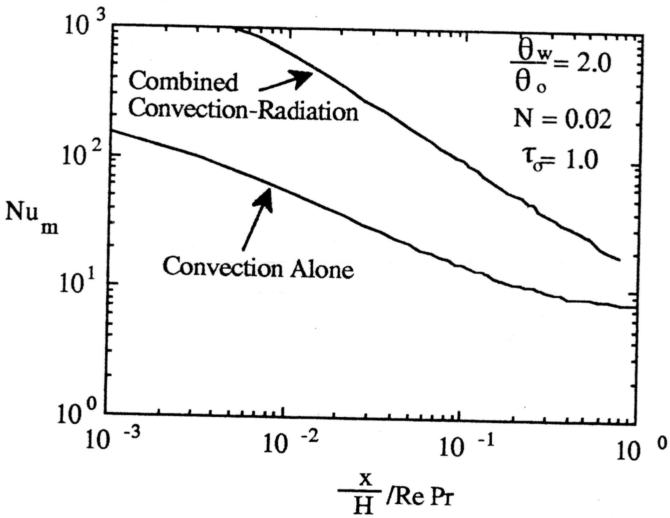

Figure 4. Average Nusselt numbers

CONCLUSIONS

In the present work, a numerical model that allows for the simulation of the combined conductive, radiative, and convective effects that take place in the entrance region of channels formed by two plane parallel plates has been presented. The numerical model is complete and removes the restrictions imposed in previous investigations.

The results from two numerical experiments where a cold fluid enters a hot channel were reported. For this preliminary study, no grid independent solution was sought and the results given are for a fixed 24 by 26 mesh. This mesh size is enough to show the validity of the model and the development of the different Nusselt numbers and bulk temperature.

Based on the results presented here, it is concluded that the numerical model produces plausible results and that the mechanism of radiative heat exchange strongly affects the heat transfer process that takes place in the entrance region of this type of channels. In view of these findings, a more detailed study aimed at finding benchmark solutions for all type of boundary conditions is recommended.

REFERENCES

[1] Sparrow, E. M., "Analysis of Laminar Forced-Convection Heat Transfer in the Entrance Region of Flat Rectangular Ducts," *NACA Tech. Note*, TN 3331, 1955.

[2] Murakawa, K., "Theoretical Solutions of Heat Transfer in the Hydrodynamic Entrance Length of Double Pipes," *Bull. JSME* 3, pp. 340-345, 1980.

[3] Stephan, K., "Wärmeübergang und Druckabfall bei Nicht Ausgebildeter Laminarströmung in Rohren und in Ebenen Spalten," *Chem. Ing. Tech.* 31, pp. 773-778, 1959.

[4] Hwang, C. L., and Fan, L. T., "Finite-Difference Analysis of Forced-Convection Heat Transfer in Entrance Region of a Flat Rectangular Duct," *Appl. Sci. Res.*, Sect. A, 13, pp. 401-422, 1964.

[5] Mercer, W. E., Pearce, W. M., and Hitchcock, J. E., 'Laminar Forced Convection in the Entrance Region Between Parallel Flat Plates," *ASME J. Heat Transfer* 89, pp. 251-257, 1967.

[6] Viskanta, R., "Interaction of Heat Transfer by Conduction, Convection, and Radiation in a Radiating Fluid," *ASME J. Heat Transfer* 85, pp. 318-328, 1963.

[7] Kurosaki, Y., "Heat Transfer by Simultaneous Radiation and Convection in an Absorbing and Emitting Medium in a Flow Between Parallel Plates," in *Proceedings of the Fourth International Heat Transfer Conference*, Vol. 3, No. R2.5, New York, Elsevier, 1970.

[8] Keshock, E. G., and Siegel, R., "Combined Radiation and Convection in a asymmetrically Heated Parallel-Plate Flow Channel," *ASME J. Heat Transfer* 86, pp. 341-350, 1964.

[9] Lin, S. T., and Thorsen, R. S., "Combined Forced Convection and Radiation Heat Transfer in Asymmetrically Heated Parallel Plate Channels," *Proceedings of the Heat Transfer and Fluid Mechanics Institute*, Stanford University Press, 1, pp. 32-44, 1970.

[10] Sánchez, A., Krajewski, W. F., y Smith, T. F., *A General Purpose Radiative Transfer Model for Application to Remote Sensing in Multi-Dimensional Systems*, IIHR Report No. 355, Iowa Institute of Hydraulic Research, The University of Iowa, Iowa City, Iowa, 1992

[11] Incropera, F. P., and De Witt, D. P., *Fundamentals of Heat and Mass Transfer*, John Wiley & Sons, New York, 1985.

[12] Patankar, S. V., *Numerical Heat Transfer and Fluid Flow*, McGraw-Hill, New York, 1980

[13] Modest, M. F., *Radiative Heat Transfer*, McGraw-Hill, New York, 1993.